Afyon Kocatepe Üniversitesi Fen ve Mühendislik Bilimleri Dergisi
Afyon Kocatepe University – Journal of Science and Engineering
https://dergipark.org.tr/tr/pub/akufemubid

Araştırma Makalesi / Research Article
e-ISSN: 2149-3367
DOI: https://doi.org/10.35414/akufemubid.1476993
AKÜ FEMÜBİD **25** (2025) 015201 (95-106)
AKU J. Sci. Eng. **25** (2025) 015201 (95-106)

Effect of 1wt% Gold Nanoparticles on the Electrical and Detection Parameters of Gold Chloride/n-Si and Gold Chloride/p-Si Photodiodes

Makale Bilgisi / Article Info
Alındı/Received: 02.05.2024
Kabul/Accepted: 03.09.2024
Yayımlandı/Published:07.02.2025

% 1 Oranında Altın Nanoparçacıklarının Altın Klorür/n-Si ve Altın Klorür/p-Si Fotodiyotlarının Elektriksel ve Ayırt Edici Parametreleri Üzerine Etkileri

Hatice KAÇUŞ *

Ardahan University, Engineering Faculty, Department of Electrical and Electronics Engineering,75002, Ardahan, Turkey

Abstract

We coated a thin film of Gold (III) Chloride dye decorated with Au nanoparticles on both n-Si and p-Si wafers using the spin-coating method. Then, metal-semiconductor (MS) devices were obtained by evaporating the schottky (Co metal) and ohmic (Al metal) contacts on the front and back surfaces of the Au nanoparticle-decorated Gold (III) Chloride film-coated wafers, respectively. Thus, Co/ Gold (III) Chloride: Au NPs /n-Si and Co/ Gold (III) Chloride: Au NPs /p-Si Schottky photodiodes were fabricated and measured with I-V measurements under dark and various light conditions at room temperature. The devices showed good rectifying behaviors and low barrier height properties. Various device parameters such as ideality factor, barrier height, and series resistance values are very important for the electrical properties of the diodes. These values are calculated and compared with each other. The Au nanoparticles (NPs)-doped devices showed good photovoltaic properties. The detection parameters demonstrated that the fabricated devices could be used for optoelectronic applications.

Keywords: *Gold ((III) Chloride; Gold Nanoparticles; Photodiode; Organic Dyes; Responsivity; Detectivity*

Öz

Spin kaplama tekniği kullanılarak hem n-Si hem de p-Si yüzeyleri Au nanoparçacık ile katkılanmış Altın (III) Klorür ince filmi ile kaplandı. Daha sonra, Au nanoparçacık katkılanmış Altın (III) Klorür filmi ile kaplı numunelerin sırasıyla ön ve arka yüzeyleri schottky (Co) ve ohmik (Al) metal kontakları buharlaştırılarak metal-yarı iletken aygıtlar elde edildi. Böylece, Co/ Altın (III) Klorür: Au NP/n-Si ve Co/ Altın (III) Klorür: Au NP/p-Si Schottky fotodiyotları elde edildi ve oda sıcaklığında karanlık ve çeşitli ışık şartları altında I-V ölçümleri yapıldı. Aygıtlar iyi doğrultma davranışları ve düşük bariyer yükseklikleri gösterdi. İdealite faktörü, bariyer yüksekliği, seri direnç değerleri gibi çeşitli aygıt parametreleri diyotların elektriksel özellikleri açısından oldukça önemlidir. Bu değerler hesaplandı ve birbirleriyle karşılaştırıldı. Au nanoparçacık ile katkılanmış aygıtlar, iyi fotovoltaik özellik gösterdi. Seçicilik parametreleri, üretilen aygıtların optoelektronik uygulamalar için geliştirilebileceğini gösterdi.

Anahtar Kelimeler: *Altın ((III) Kloride; Altın Nanoparçacık; Fotodiyot; Organik Boyalar; Duyarlılık; Ayırt Edicilik (Seçicilik)*

1. Introduction

Recently, the hybrid materials consisting of a mixture of organic and inorganic materials have allowed the emergence of a new field such as hybrid optoelectronic devices (Aslam Manthrammel et al. 2019). Particularly, the combination of devices such as photodiodes, organic or hybrid dye-sensitized solar cells and materials such as highly conductive polymers or developing inorganic semiconductor has led to serious research (Jackle et al. 2015). In recent studies, the photodiode come to the fore among the devices produced using hybrid materials.

Photodiodes (PDs) are photosensors with Schottky, p-n and p-i-n junction structures that convert incoming photon energy into electricity. When the photodiode is excited by photon with higher energy than band gap, electron-hole pairs are produced by light illumination inside the space charge region. Then, electron-hole pairs produced by photons are separated by electric field of junction and thus, preventing recombination of photo-generated pairs. Then, these charges are drifted by electric field of junction and the photocurrent is accomplished (Tataroğlu et al.2016). The incorporation of a new interfacial layer between metal-semiconductor such as an organic dye or an insulating layer opens significant opportunities for the formation of hybrid structures and fabrication of optoelectronic devices (Kacus et al.2020). The interfacial layer separating metal and semiconductor surfaces prevents diffusion and reactions at the interface.

*Sorumlu Yazar/Corresponding Author: Hatice KAÇUŞ e-posta/e-mail: haticekacus@ardahan.edu.tr

In recent years, important researches have been revealed on devices consisting of metal-semiconductor hybrid structures integrated with organic interface layers used in applications such as photodiode (PD), photovoltaic (PV) cells, FETs, and LEDs (Taşçıoğlu et al. 2010, Ameline et al. 2015). However, the obtained new photodiodes differ from ideal devices due to the inhomogeneities caused by the interface, changing series resistance, and the extra energy distribution states forming at the interface. The interface of metal-semiconductor structures can be developed using a variety of techniques such as organic dye layer. Organic dye materials with low cost and easy manufacturing procedures (Ikram et al. 2015, Akkaya et al. 2019) improve device performance and also electrical characteristics of metal-semiconductor structures. For instance, organic dyes can increase or decrease device parameters such as the ideality factor (n), schottky barrier height (Φ_b), and series resistance (R_s) (Akkılıç et al. 2006, Yüksel et al. 2013).

Technical methods (maceration, distillation, fermentation, decantation, precipitation, and filtering) have widely used in the production of organic dyes obtained from flowers, seeds, fruits, bark, root of plants and insects (Santos et al. 2018). Gold (III) Chloride, traditionally known as auric chloride, consists of gold and chlorine. Gold (III) Chloride has molecular formula Au_2Cl_6 (Büche et al. 2008) and solvent in water as well as ethanol. It has a square planar and decomposes temperature (over 160 ◦C) or varying light conditions. The bonding in Gold (III) Chloride dye has accepted somewhat covalent (Clark et al.1958).

Moreover, energy band and chemical bonding structures of organic materials can be easily modified. Thus, these materials are often preferred in excellent performance photodiode (PDs) devices. The noble metal (Au, Ag and Pt) nanoparticles can be done with this modification. These noble metal nanoparticles show surface plasmon resonance behavior and thus, exhibit near-field effects around particles due to the collective oscillations of conduction electrons (Kacus et al.2019, Kacus et al. 2021, Kacus et al.2020). Such oscillations result from coupling the incident radiation with the of vibrational frequency of the metal nanoparticles when wavelength of the radiation is bigger compared to the size of the metal nanoparticles (Zhang et al.2008, Spinelli et al. 2012). The doping metal nanoparticles into the organic interface layer can improve the optical and electrical properties of metal-insulator-semiconductor (MIS) devices. These properties may be manipulated by changing the shape or size of the noble metal nanoparticles and dielectric parameters of the environment (Kelly et al.2003, Mock et al. 2002). Theoretically, it is proven that altering geometry of metal nanoparticles can tune the resonance wavelength and thus, complex nanostructures can be form increasingly sharp and strong resonance (Kottmann et al. 2001). Photon scattering from metal nanoparticles increases the optical path length of the incident light and thus, this case improves the effective optical thickness in the active or interface layer of the electronic devices.

Theoretical and experimental studies have reported the importance of organic dyes, the fabrication and improving of metal-semiconductor devices in the literature. In previous studies, Kacus et al. (2021) obtained Co/Aniline Blue: Au NPs/*n*-Si/ Al device and investigated electrical properties under dark and various light conditions (range from 100-400 mW/cm^2). The reverse bias current increased depending on increasing light values, and this confirmed the photodiode behavior in the study.

The ideality factor (n) and schottky barrier height (Φ_b) in values of the Co/Aniline Blue/*n*-Si/ Al were reported as 2.12 and 0.60 eV while they were obtained as 1.93 and 0.72 eV for Co/Aniline Blue:AuNPs/*n*-Si/ Al, respectively. The doping Au NPs into the Aniline Blue interlayer affected device parameters such as decreasing of n value and increasing of Φ_b value. Ganesh et al. (2018) obtained indigo carmine photodiode and applied wide range voltage and frequencies for optoelectronic applications. Seo et al. (2011) investigated the photovoltaic properties of coumarin dyes containing a low-band- gap chromophore of ethylenedioxythiophene (EDOT) and also calculated fill factor and efficiency as 0.70 and 6.07% under irradiation (the standard AM 1.5).

Özkartal et al. (2019) fabricated photodiode as using Methyl Violet organic interlayer and electrical properties of photodiode were calculated. It has been found that methyl violet dye modified the barrier height of diodes. Reem et al. (2018) obtained Al/coumarin/p-Si/Al diode and the high photoresponse properties of this device have resulted to be used as photodiode device. Koçyiğit et al. (2021) obtained Co/CR:Au/n-Si and Co/CR:Au/p-Si Schottky photodetector and these devices have the characteristics of I-V measurements under dark and various light power (at room temperature) conditions. The obtained devices exhibited both good rectifying and low barrier height properties. The fabricated two devices can be preferred for photodiode and photodetector technology. Cavusoglu et al. (2024) studied the electrical properties of the Al/Au:CuO/n-Si device using current–voltage (*I*–*V*) measurements for various light power densities. These heterojunctions exhibited good photodiode behavior. Responsivity and specific values of

heterojunction device are 3.44 A/W and 1.58×10^{10} Jones for the 2% Au-doped CuO interfacial layer.

In the present work, Gold (III) Chloride: Au NPs interface was used to form an effective hybrid photodiode between Co and n-Si layers. Spin coating method was used this work for being simple, low cost and convenient. According to literature studies, there is no work for fabrication and investigating the electrical measurements of this hybrid structures. Thus, we aim to analyze the potential use of Gold (III) Chloride: Au NPs material for photodiode technology and current-voltage measurement of device was performed under the various light intensity and dark conditions, respectively. The responsivity and photosensitivity parameters of n-Si and p-Si substrates photodiodes were compared in detail.

2. Materials and Methods

2.1 Cleaning of Si-Substrate and creation of front and back contacts

Gold (III) Chloride dye and Au NPs were obtained from Sigma-Aldrich and 0.1 g of Gold (III) Chloride was dissolved in 10 ml of water, and then Au NPs (1wt%) were doped with Gold (III) Chloride solution to obtain a mixture of Gold (III) Chloride: Au NPs. This mix was stirred with a magnetic stirrer for 12 h at room condition (25 °C). N-Si and p-Si semiconductor used in this study have a thickness of 400 µm, carrier concentration of 7.5 $x10^{16}$ cm^{-3}, orientation of 100, and resistivity of 5-10 Ω-cm. These substrates were divided into 1cm^2 pieces and cleaned using the RCA procedure as described in Kacus et al. (2020). Following chemical cleaning procedure has been used for n-Si and p-Si wafer (Kacus et al. 2020):

- $NH_3+H_2O_2+6H_2O$, 60 °C, t=10min (RCA1).
- Deionised water rinse.
- $HCl+ H_2O_2+6H_2O$, 60 °C, t=10min (RCA2)
- Deionised water rinse.
- Drying in N_2 gas.

After cleaning, back (ohmic) contact (Aluminium, Al, metal) of n-Si and p-Si wafers were formed with using thermal evaporation system at ~10^{-6} Torr pressure. These ohmic contact substrates (n-Si and p-Si wafers) have annealed in an N_2 environment (5 min and 15 min) to provide ohmic contact with low resistance, respectively. Then, Gold (III) Chloride:Au NPs mixture was covered on the brilliant surfaces of the Si wafers by a spin coating (3000 rpm and 50 s) and left to dry. After this coating process, schottky contact (Cobalt, Co metal) was formed on thin film by VAKSIS DC magnetron sputtering by using an array of mask with 7.85 $x10^{-3}$ cm^2 opening areas for the obtaining rectifying contact. As a result, the Co/ Gold (III) Chloride: Au NPs /n-Si and Co/ Gold (III) Chloride: Au NPs /p-Si hybrid structure photodiodes were completed and the schematic illustration of the hybrid structure devices are shown in Figure 1.

2.2 Equipment and measurements

The electrical I-V measurements of the obtained hybrid structure photodiodes were formed by Keithley 2400 Picoammeter/Voltage Source under the dark conditions. The Sciencetech solar simulator (AM1.5) was used to determine the effect of light on the device parameters (range from 100-400 mW/cm^2).

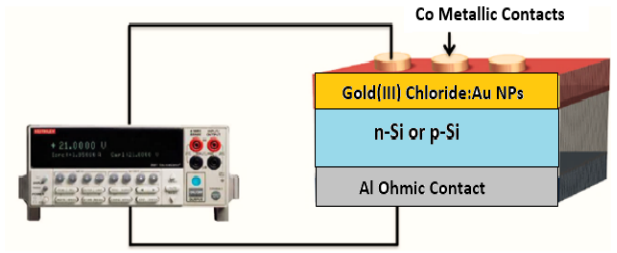

Figure 1. Schematic illustration of the Co/Gold (III) Chloride:AuNPs/n-Si and Co/Gold (III) Chloride:AuNPs /p-Si photodiodes.

3. Results and Discussions

lnI-V plots of the Co/Gold (III)Chloride /n-Si, Co/Gold (III) Chloride:AuNPs /n-Si, Co/Gold (III)Chloride /p-Si and Co/Gold (III) Chloride:AuNPs /p-Si photodiodes have been shown in Figure 2a and b to understand the effect of Au nanoparticles on different semiconductor types photodiodes at ± 2V, respectively. The current was decreased with Au NPs for Co/ Gold (III) Chloride: Au NPs /n-Si and Co/ Gold (III) Chloride: Au NPs /p-Si photodiodes at reverse bias and under the dark conditions. After the interface layer is doped with Au NPs, the current decreases at the reverse bias voltage, and this can be explained by electron-hole recombination as a function of charge carriers and low minority carrier concentration (Kacus et al. 2021). Furthermore, the Co/ Gold (III) Chloride: Au NPs /n-Si photodiode exhibited clearly a large current shift. These differences can be attributed to the work functions of Co metal, n-type Si semiconductor, p-type Si semiconductor, and Au NPs, which are 5 eV, 4.05 eV, 5.15 eV and 3.6eV, respectively (Yılmaz et al. 2020). Since the work function of the n-Si semiconductor is closer to Co metal, rectifying contact can occur easily between the Co metal and n-Si type semiconductor. Gold (III) Chloride and SiO_2 (native oxide) layers on the Si wafers can help to form rectifying contact but, the rectifying contact can not occur easily between Co metal and p-Si semiconductor (Zandonay et al. 2008). Various device parameters such as ideality factor (n), schottky barrier height (Φ_b) as well as series resistance (R_s) values were obtained from I-V characteristics of both

photodiodes. After Au NPs doped to Gold (III) Chloride dye, Co/ Gold (III) Chloride: Au NPs/n-Si photodiode showed better performance than Co/Gold (III) Chloride:AuNPs /p-Si, Co/Gold (III)Chloride /n-Si and Co/Gold (III)Chloride /p-Si photodiodes. Firstly, the thermionic emission theory (TE) was employed to obtain the n and Φ_b values. Then, these calculated values for all photodiodes are listed in Table 1 under the dark condition.

Equations of thermionic emission theory is given as below (Kacus et al. 2020):

$$I = I_0 \left[\exp\left(\frac{qV}{nkT}\right) - 1\right] \quad (1)$$

The T, q, V, k, I_0 and n terms are temperature, charge of electron, the applied voltage, boltzmann constant, saturation current and ideality factor, respectively.

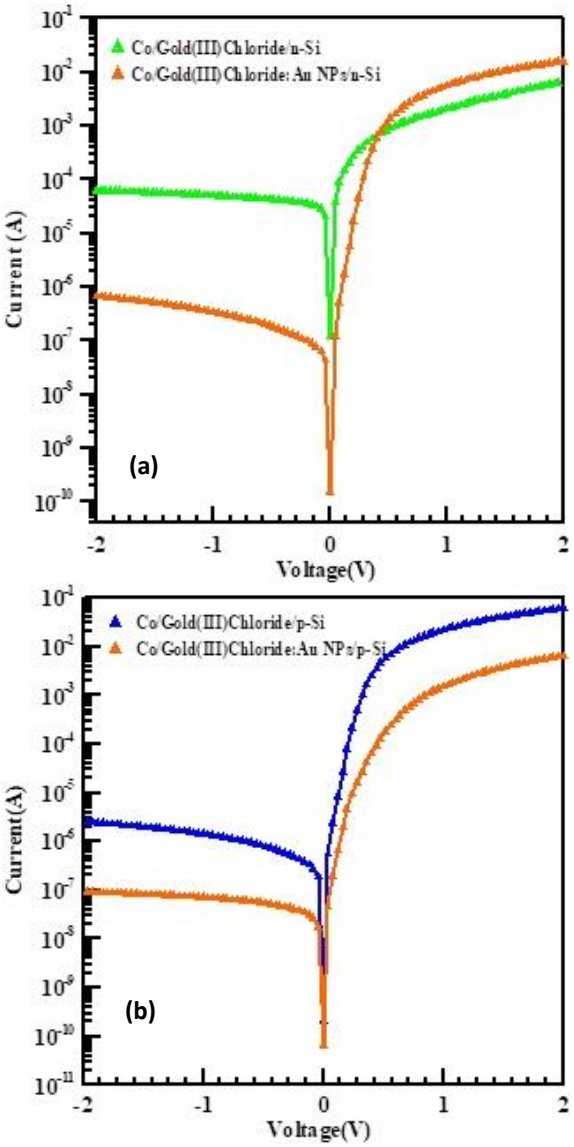

Figure 2. Semi-logarithmic I-V characteristics of the **a)** Co/Gold (III)Chloride /n-Si, Co/Gold (III) Chloride: AuNPs /n-Si and **b)** Co/Gold (III)Chloride /p-Si, Co/Gold (III) Chloride:AuNPs /p-Si photodiodes under dark condition.

The barrier height values are calculated from saturation current (I_0) equation and are given as below:

$$I_0 = AA^*T^2 \exp\left(\frac{-q\Phi_b}{kT}\right) \quad (2)$$

where A (7.85 x 10^{-3} cm^2 for n-type Si), A*(112 A/cm^2K^2 for n-type Si and 11 A/cm^2K^2 for p-type Si) and the barrier height (Φ_b) are effective diode area, Richardson constant and barrier height of zero bias, respectively. The formulas of idealite factor (n) and barrier height (Φ_b) values are given as below (Kacus et al. 2020):

$$n = \frac{q}{kT}\left(\frac{dV}{d(\mathrm{In}I)}\right) \quad (3)$$

$$\Phi_b = \frac{kT}{q} \mathrm{In}\left(\frac{AA^*T^2}{I_0}\right) \quad (4)$$

The n and Φ_b values of the Co/Gold (III)Chloride /n-Si device were calculated as 5.89 and 0.54 eV and also, these values were determined as 1.50 and 0.71 eV for Co/Gold (III) Chloride:AuNPs /n-Si device, respectively. While the n and Φ_b values of the Co/Gold (III)Chloride /p-Si device were determined as 1.74 and 0.62 eV, these values have calculated as 1.92 and 0.69 eV for Co/Gold (III) Chloride:AuNPs /p-Si device. The ideality factor and barrier height values are slightly different for Co/Gold (III) Chloride /n-Si and Co/Gold (III) Chloride : Au NPs /n-Si devices than for Co/Gold (III)Chloride /p-Si and Co/Gold (III) Chloride : Au NPs /p-Si devices due to the work function differences of the n-type Si and p-type Si semiconductor wafers. These experimental results can be expressed with metal-semiconductor (M-S) interfaces and the different work function of different type semiconductor (Kacus et al. 2021). The ideal factor of ideal rectifying device is unity and also, various effects such as series resistance, the inhomogeneous of interface layer and the presence of oxide layer on semiconductor wafers cause the ideality factor to be higher than ''1'' [30]. The experimental results reported that Au NPs into the Gold (III) Chloride layer effected device parameters. Hence, presence of noble metals nanoparticles in the interface layer of the device can change the inhomogeneity of schottky barrier height. The current transport mechanism is a temperature-dependent process across the metal-semiconductor (M-S) interface and low temperatures cause a decrease in schottky barrier height resulting in electrons can surmount the lower barrier height. When a large number of electrons gain enough energy at high temperature conditions, they can overcome high barrier heights (Bilgili et al. 2019). At room temperature, the decrease in n values can be

attributed to a reduction in the defect state density and the increased surface roughness at the metal-dielectric interface due to the incorporation of Au NPs into the device and the increase of R_s values. Additionally, the n value of device with the plasmonic layer is significantly decreased compared to the value of the device with the gold chloride layer at higher temperature and this case can affect electronic properties of device. Moreover, this situation can be explained by the decrease in interfacial defect states and the increase in free carrier concentration across the metal-semiconductor junction (Gayen et al. 2014).

Another method used to confirm the results of device parameters obtained from the thermionic emission (TE) theory is the Norde method (Norde, 1979). The Norde function plots of the Co/Gold (III)Chloride /n-Si, Co/Gold (III) Chloride:AuNPs /n-Si , Co/Gold (III)Chloride /p-Si and Co/Gold (III) Chloride:AuNPs /p-Si photodiodes are shown in Figure 3, respectively. The obtained photodiodes demonstrated a characteristic behavior such as normal Norde function. The following formula expresses the Norde function:

$$F(V) = \frac{V}{\gamma} - kT\left(\frac{I}{AA^{*}T^{2}}\right) \quad (5)$$

The γ is an integer which is higher than n. Then, the F (V) versus V plot of these devices is drawn and the minimum value of this plot is shown in the $\mathrm{F(V)} - \mathrm{V}$ plot.The next stage, Eq.6 is used to calculate barrier height (Φ_b) value:

$$\Phi_{\mathrm{b}} = \mathrm{F(V}_m) + \left(\frac{V_m}{\gamma} - \frac{kT}{q}\right) \quad (6)$$

where $F(V_m)$ and V_m are the minimum values of F(V) and the corresponding voltage, respectively. Then, experimental serial resistance $(\mathrm{R_s})$ value is obtained from the following Eq.7:

$$R_s = \frac{kT}{q}\frac{\gamma - \mathrm{n}}{I_{min}} \quad (7)$$

The barrier height (Φ_b), series resistance (R_s) and rectifying ratio(RR) values for obtained devices are listed in Table 1. The rectifying ratio (RR) values increased for the Co/ Gold (III) Chloride: Au NPs /n-Si (D2) and Co/ Gold (III) Chloride: Au NPs /p-Si (D4) photodiodes with Au nanoparticles (NPs)-doped devices.

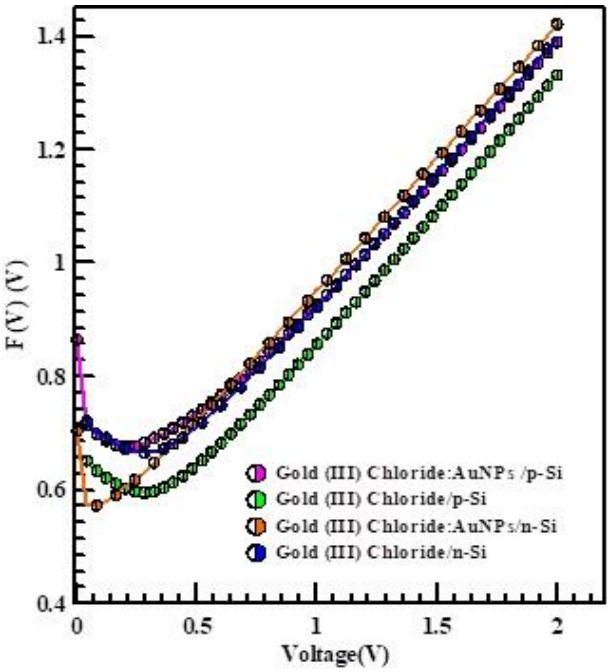

Figure 3. Norde plots of F(V) vs V of Co/Gold (III)Chloride /n- Si, Co/Gold (III) Chloride:AuNPs /n-Si , Co/Gold (III)Chloride /p-Si and Co/Gold (III) Chloride:AuNPs /p-Si photodiodes.

Table 1 Various device parameters of Co/Gold (III)Chloride /n-Si Co/Gold (III) Chloride:AuNPs /n-Si , Co/ Gold (III)Chloride /p-Si and Co/Gold (III) Chloride:AuNPs /p-Si photodiodes

	I-V		dV/d(lnI)		H(I)-I		Norde		
Device Structure	**n**	**Φ_b (eV)**	**n**	**R_s(Ω)**	**R_s(Ω)**	**Φ_b (eV)**	**Φ_b (eV)**	**R_s(Ω)**	**Rectifying Ratio(RR)**
Gold (III)Chloride /n-Si	5.89	0.54	10.43	156.83	158.71	0.51	0.57	32.21	104.29
Gold (III) Chloride:AuNPs /n-Si	1.50	0.71	1.78	86.69	86.86	0.67	0.77	108.7	22720
Gold (III)Chloride /p-Si	1.74	0.62	1.74	24.83	24.90	0.69	0.47	13.30	23345
Gold (III) Chloride:AuNPs /p-Si	1.92	0.69	3.71	173.20	176.70	0.65	0.51	435.1	64330

The determined ideality factor and barrier height values by other methods are in good agreement with obtained parameters from the thermionic emission theory. Another technique used to comfirm the calculated device parameters is Cheung method (Cheung et al. 1986). The dV/d(lnI) and H (I) are two Cheung functions and thus, they exhibit straight lines when the functions are plotted against current. The n, Φ_b, and two R_s values were determined using these plots. The determination of the device parameters with these plots has been reported in previous studies (Koçyiğit et al. 2019). In this method, serial resistance (R_s) value of the device is expressed as below:

$$\frac{\mathrm{dV}}{\mathrm{dIn(I)}} = \frac{\mathrm{nkT}}{\mathrm{q}} + \mathrm{IR_s} \quad (8)$$

$$H(I) = V - n\frac{kT}{q} In\left(\frac{I}{AA^*T^2}\right) \quad (9)$$

and

$$H(I) = IR_s + n\Phi_b \quad (10)$$

The Cheung plots of the obtained Co/Gold (III)Chloride /n-Si, Co/Gold(III) Chloride:AuNPs/n-Si, Co/Gold (III)Chloride /p-Si and Co/Gold (III) Chloride:AuNPs /p-Si devices are demonstrated in Figure 4a and b for dark condition, respectively. The Cheung plots exhibited good linearity for the obtained photodiodes. The calculated n, Φ_b, and two R_s values are shown in Table 1 for the obtained photodiode devices. The determined device parameters confirm the correction of the results and these values are in harmony with the obtained results with other techniques (Luongo et al. 2017). The metal nanoparticles doping with organic materials caused the formation of agglomerations due to the potential attractive forces between Gold (III) Chloride and metal nanoparticles (Coetzee et al. 2020) and thus, this case led to increase series resistance values. The agglomeration around metal nanoparticles can cause higher resistance for the Co/Gold (III) Chloride : AuNPs /p-Si device resulting in doping Au nanoparticles in the Gold (III) Chloride solution. According to the obtained results, Au NPs doped into interface layer may affect the distribution of the interface states of metal-insulator-semiconductor (MIS) structures. The new interfacial states, such as oxide-organic interface states, can be formed by chemical interactions between interface layer and n-Si surface.

The I-V graphs of the obtained Co/Gold (III) Chloride:AuNPs /n-Si and Co/Gold (III) Chloride:AuNPs /p-Si devices are demostrated in Figure 5a and b under dark and various light conditions at ±1V, respectively. The fabricated devices exhibited normal diode behavior due to current passage at forward biases and current blockage at reverse biases (Ejderha et al. 2009). When photodiodes are exposed to light, the current increases in the reverse bias voltage under various light power densies due to characteristics of photodiodes. It can produce photocurrent when energies of photons are higher than schottky barrier height. The photodiode devices composed of Au nanoparticles are shown in Figure 5a and b. In this approach, the produced photocurrent are directly related to the plasmonic properties of different metal nanoparticles. When thin Gold (III) Chloride:Au NPs layer used as the active layer, it absorbs the incident light and free carriers are produced and also, charges separated due to the electric field's influence at the Co/Gold (III) Chloride: Au NPs/n-Si or Co/Gold (III) Chloride: Au NPs/p-Si interface.

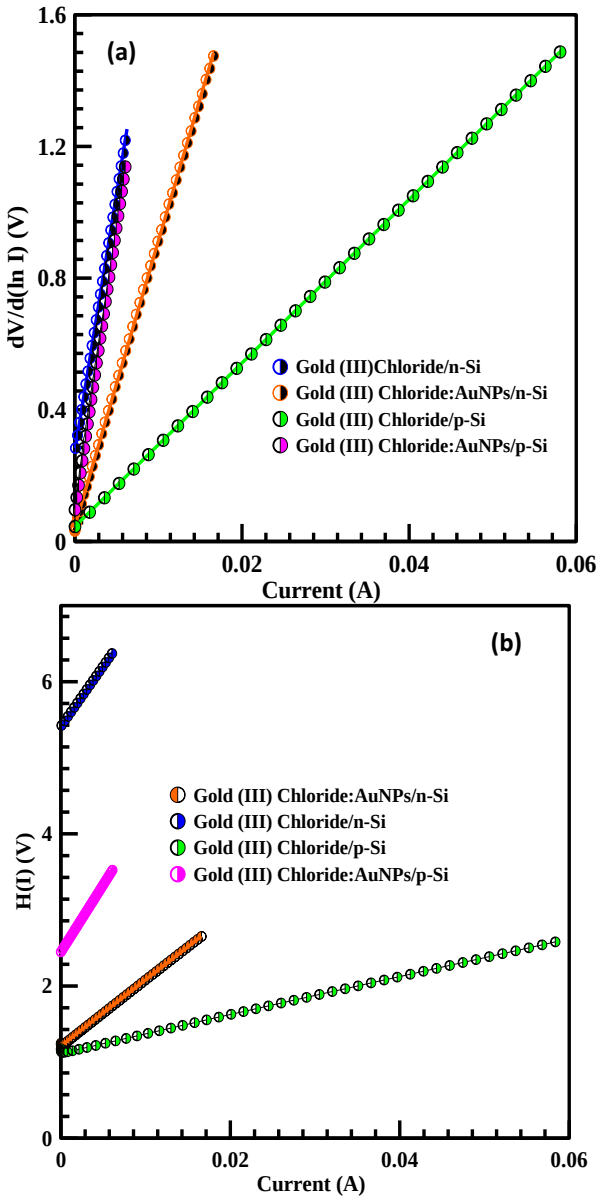

Figure 4. Cheungs plots of dV/dln(I) - I **(a)** and H(I) - I **(b)** of Co/Gold (III)Chloride /n-Si, Co/Gold (III) Chloride:AuNPs /n-Si, Co/ Gold (III)Chloride /p-Si and Co/Gold (III) Chloride:AuNPs /p-Si photodiodes.

The built-in field in the reverse bias leads electrons to be instantly transfered from the Co/Gold (III) Chloride: Au NPs/n-Si structure to n-Si semiconductor. While holes are transported in the Gold (III) Chloride:Au NPs layer toward the Co electrode, electrons are collected by the Al electrode. Thus, the reverse current value effectively increased than the dark current due to the generation of free carriers (El-Nahass et al. 2007). In the dark condition, electrons can pass through lower barriers due to the inhomogeneity of the Gold (III) Chloride:Au NPs/n-Si interface. Therefore, the current preferentially flows through the patches with lower barriers (Φ_b). When some electrons are exposed to light, they gain high energy and thus, the excited electrons gain enough energy to overcome a larger barrier. This case may lead to an

increase in the Φb value and a decrease in the n value (Budak et al.2020, Kaplan et al. 2021)and also, Table 1 can be listed.

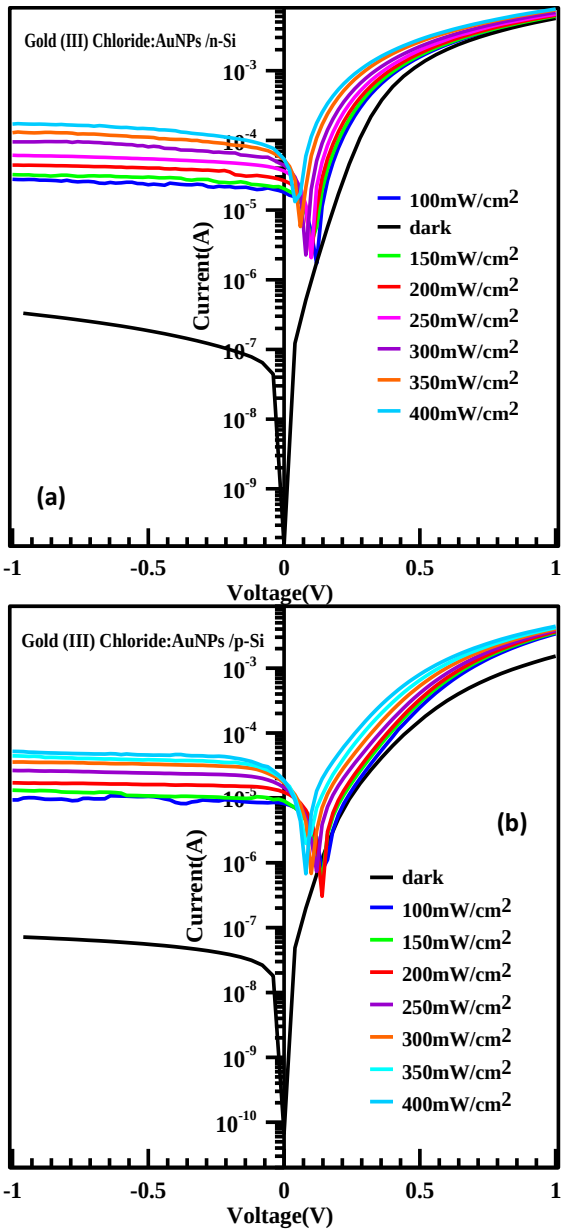

Figure 5. Semi-logarithmic *I–V* characteristics of the **a)** Co/Gold (III) Chloride : Au NPs /n-Si and **b)** Co/Gold (III) Chloride : Au NPs /p-Si photodiodes under various light conditions.

The Co/Gold (III) Chloride:AuNPs /n-Si photodiode has lower dark reverse current and higher photocurrent than the Co/Gold (III) Chloride:AuNPs /p-Si photodiode due to close work functions of n-Si and Co element at a certain light power. When the obtained Co/Gold (III) Chloride:AuNPs /n-Si and Co/Gold (III) Chloride:AuNPs /p-Si photodiodes are exposed to light, the forward bias current does not change so much depending on increasing light power. The difference in work function of n-type and p-type semiconductor can be attributed to the difference in forward and reverse bias currents. The reverse bias current of the Co/Gold (III) Chloride: Au NPs /n-Si and Co/Gold (III) Chloride: Au NPs /p-Si photodiodes increased with increasing light power. However, reverse current shows a flat profile with increasing light at reverse biases. When photodiodes are exposed to light, it causes an increase in the charge carriers at the interface and a change in the minimum current values at the forward bias region, and thus the devices exhibited photovoltaic behavior (Tatar et al.2009).

The responsivity (R) is an important parameter and the input-output gain of the device is determined with this value (Gayen et al. 2014). The rectifying ratio (RR) (for a certain voltage value), responsivity (R), and specific detectivity (D*) formulas are given as follows:

$$RR = \frac{I_{forward}}{I_{reverse}} \tag{11}$$

$$R = \frac{I_p}{PA} \tag{12}$$

$$D^* = R\sqrt{\frac{A}{2qI_{dark}}} \tag{13}$$

where I_p is photocurrent, P is incident power density, and A is the effective area of detector. The photodiode parameters such as rectifying ratio (RR), photocurrent (I_{ph}), responsivity (R), and specific detectivity (D*) of Co/Gold (III) Chloride:AuNPs /n-Si and Co/Gold (III) Chloride:AuNPs /p-Si photodiodes are listed in Table 2 and 3 with the increasing light power intensity, respectively. Other important parameters such as detectivity (D*), responsivity (R), rectifying ratio (RR) and photocurrent (I_{ph}) also characterize a photodiode. In Fig. 6a,b,c and d detectivity (D*), responsivity (R), rectifying ratio (RR) and photocurrent (I_{ph}) profiles of the Co/ Gold (III) Chloride: Au NPs /n-Si and Co/ Gold (III) Chloride: Au NPs /p-Si photodiodes with the various light intensities are shown. The rectifying property of Co/Gold (III) Chloride:AuNPs /n-Si and Co/Gold (III) Chloride:AuNPs /p-Si photodiodes decreased in the light conditions due to increased charge transport at reverse biases in the interface while the obtained photodiodes have shown good rectifying behaviors in the dark condition (Orak et al. 2018) As the light power intensity increased, the reverse biases current increased, and thus RR values of the obtained photodiodes decreased (Yildiz et al.2020). The photodiode behaviors of the obtained Co/ Gold (III) Chloride: Au NPs /n-Si and Co/ Gold (III) Chloride: Au NPs /p-Si junctions clearly confirm this case. The RR values decreased for the Co/ Gold (III) Chloride: Au NPs /n-Si and

Co/ Gold (III) Chloride: Au NPs /p-Si photodiodes with the various light power. The RR values of the Co/ Gold (III) Chloride: Au NPs /p-Si photodiode is higher than the Co/ Gold (III) Chloride: Au NPs /n-Si photodiode. This decrease in RR values depending on increasing light power confirmed the photodiode behavior of the fabricated devices. The responsivity of all photodiodes increased depending on increasing light power. The responsivity values of the Co/ Gold (III) Chloride: Au NPs /n-Si photodiode were almost four times higher than that of the Co/Gold (III) Chloride: Au NPs /p-Si photodiode. The photocurrent values increased almost linearly depending on increasing light power intensity for Co/Gold (III) Chloride:AuNPs /n-Si and Co/Gold (III) Chloride:AuNPs /p-Si photodiodes, but the photocurrent values of the Co/Gold (III) Chloride:AuNPs /n-Si photodiode were slightly higher than that of the Co/Gold (III) Chloride:AuNPs /p-Si photodiode. The responsivity (R) and specific detectivity (D*) values of the Co/Gold (III) Chloride:AuNPs /n-Si photodiode were higher than that of the Co/Gold (III) Chloride:AuNPs /p-Si photodiode. The doping of Au NPs into the interface improves good stability of photodiode depending on the increase in light power intensity and this case is beneficial for performance. The responsivity (R) and detectivity (D*) values of the obtained photodiodes are in good agreement with the calculated values in the literature (Shafique et al.2019, Gao et al. 2019). Furthermore, ON/OFF Ratios of the Co/Gold (III) Chloride:AuNPs /n-Si and Co/Gold (III) Chloride:AuNPs /p-Si photodiodes are shown in Table 2 and 3, respectively. The change of ON/OFF ratios with light intensity is just like the change of photocurrent. The changes in both Table 2 and 3 show that the density of photo-generated carriers increases with increasing light intensity and these Co/Gold (III) Chloride:AuNPs /n-Si and Co/Gold (III) Chloride:AuNPs /p-Si devices are a suitable design for high-performance photodiode applications.

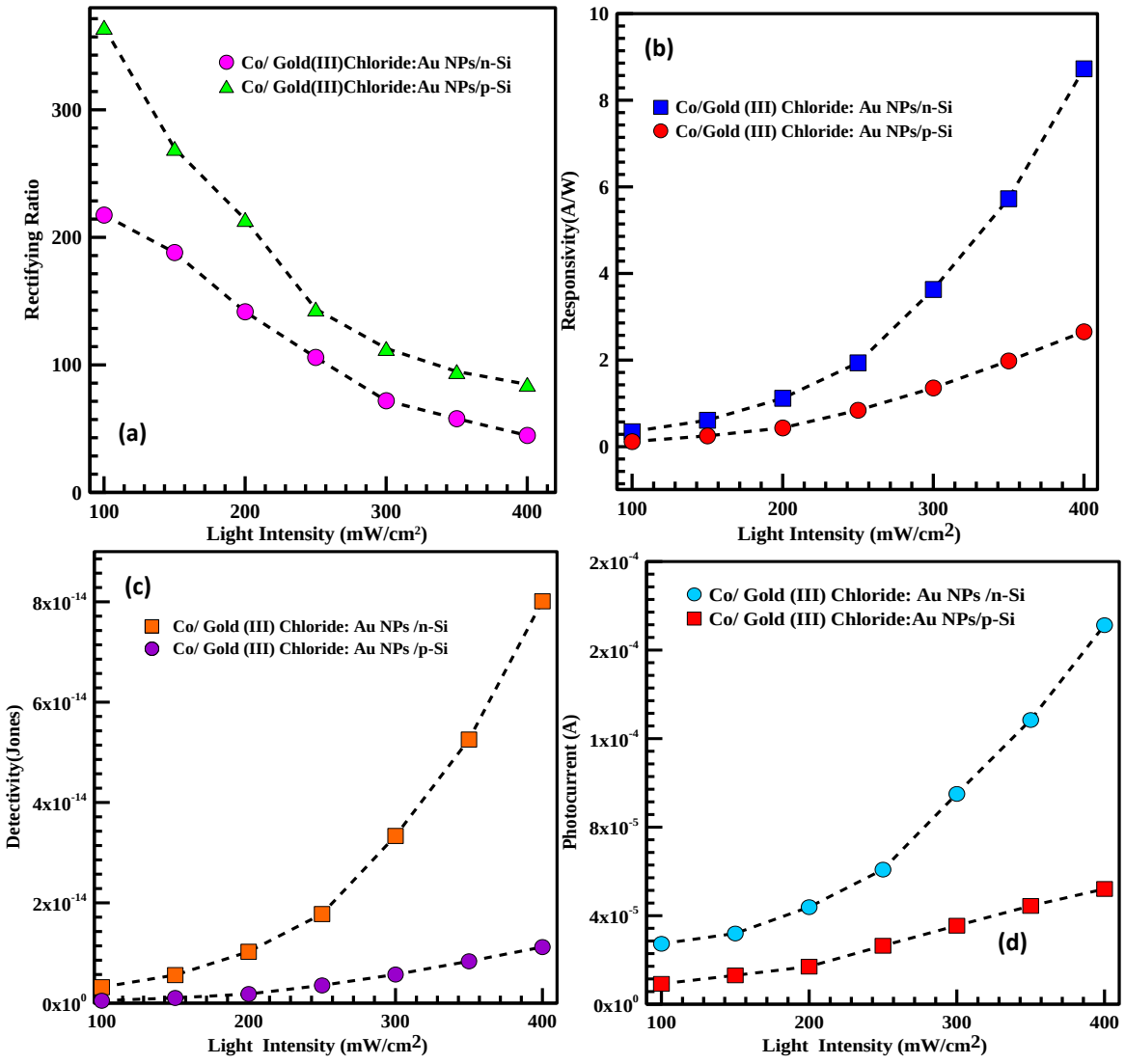

Figure 6. a) Rectifying Ratio, **b)** Responsivity, **c)** Detectivity and **d)** Photocurrent plots of the Co/ Gold (III) Chloride:Au NPs /n-Si and Co/ Gold (III) Chloride: Au NPs /p-Si photodiodes depending on the various light intensies.

Figure 7 depicts the ON/OFF Ratio reverse light intensity plots of the Co/ Gold (III) Chloride:Au NPs /n-Si and Co/Gold (III) Chloride:Au NPs /p-Si photodiodes. The ON/OFF ratio of the Co/Gold (III) Chloride:AuNPs /n-Si photodiode changed from 79.52 (100 mW/cm^2) to 498.65 (400 mW/cm^2). The ON/OFF ratio of the Co/Gold (III) Chloride:AuNPs /p-Si photodiode changed from 127.28 (100 mW/cm^2) to 718.58 (400 mW/cm^2). Experimental results showed that Au NPs made a significant improvement on the photodiodes. This situation can be explained that Au NPs with surface plasmon resonance (LSPR) affected significantly the sensitivity of the Gold (III) Chloride:AuNPs /n-Si and Gold (III) Chloride:AuNPs /p-Si photodiodes depending on light intensity. The Gold (III) Chloride: Au NPs interface material has shown different responses at various wavelengths or energy values, and these responses may enable its use in optoelectronics under various light intensities.

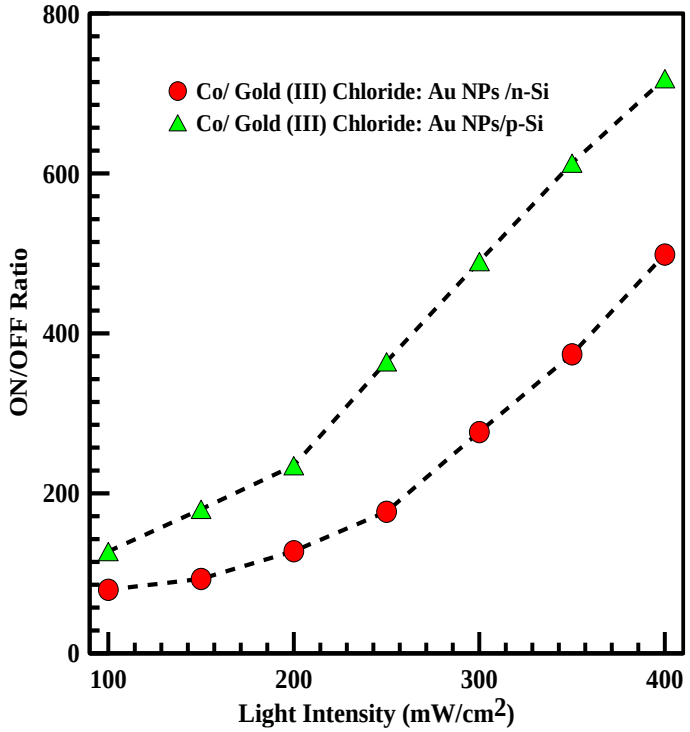

Figure 7. The ON/OFF Ratio versus light intensity for the Co/Gold (III) Chloride:AuNPs /n-Si and Co/Gold (III) Chloride:AuNPs /p-Si photodiodes.

Table 2 The detector parameters of Co/Gold (III) Chloride:AuNPs /n-Si photodiode at ±1V

Light Intensity (mW/cm^2)	I_{ph}	I_{dark}	ON/OFF Ratio	Responsivity (R)	Detectivity (D)	Rectifying Ratio(RR)
100	2.73E-05	3.4E-07	79.52	0.347	3.19E-15	217.5
150	3.19E-05	3.4E-07	93.091	0.610	5.61E-15	188.1
200	4.38E-05	3.4E-07	127.74	1.117	1.03E-14	141.6
250	6.08E-05	3.4E-07	177.08	1.937	1.78E-14	105.8
300	9.50E-05	3.4E-07	276.67	3.631	3.33E-14	71.90
350	0.000128	3.4E-07	373.92	5.726	5.26E-14	57.80
400	0.000171	3.4E-07	498.65	8.727	8.01E-14	44.70

Table 3 The detector parameters of Co/ Gold (III) Chloride:AuNPs /p-Si photodiode at ±1V

Light Intensity (mW/cm^2)	I_{ph}	I_{dark}	ON/OFF Ratio	Responsivity (R)	Detectivity (D)	Rectifying Ratio(RR)
100	9.22E-06	7.2E-08	127.28	0.117	4.96E-16	364.77
150	1.30E-05	7.2E-08	180.14	0.249	1.05E-15	269.79
200	1.70E-05	7.2E-08	234.69	0.433	1.83E-15	214.08
250	2.64E-05	7.2E-08	364.58	0.841	3.55E-15	143.8
300	3.55E-05	7.2E-08	489.85	1.356	5.72E-15	112.9
350	4.44E-05	7.2E-08	612.95	1.980	8.35E-15	94.80
400	5.20E-05	7.2E-08	718.58	2.654	1.12E-14	84.70

4. Conclusion

The Gold (III) Chloride: Au NPs and Gold (III) Chloride were used as interlayer in between Co metal and both n-type and p-type silicon, and also these layers were covered with spin coating technique for obtained Co /Gold (III) Chloride: Au NPs /n-Si, Co/Gold (III) Chloride: Au NPs /p-Si, Co/Gold (III) Chloride/n-Si and Co/Gold (III) Chloride/p-Si photodiodes. The I-V measurements of the photodiodes were compared with each other and characterized under the dark and light conditions. The diode parameters were calculated from Thermionic Emission theory, Norde and Cheung methods using I-V measurements for dark conditions and were discussed of detail. The calculated serie resistance values are suitable for both undoped and Au-doped devices. The photovoltaic parameters such as photocurrent, responsivity and detectivity values were obtained and compared with Co/Gold (III) Chloride:AuNPs /n-Si and Co/Gold (III) Chloride:AuNPs /p-Si photodiodes. The rectification ratio (RR) of the fabricated photodiodes decreased with the increase of light power density, and thus the devices show good rectification properties. The Au-doped photodiodes demonstrated linear photocurrent (Iph) behavior, good responsivity property (R) and detectivity property (D*) such as a typically photodiode. The responsivity (R) and detectivity (D*) values of the Co/Gold (III) Chloride:AuNPs /n-Si photodiode slightly increased with increasing light power intensity while the Co/Gold (III) Chloride:AuNPs /p-Si photodiode almost stayed constant. It was emphasized that these two photodiodes could be used in theindustry based on the obtained experimental results. Although th The rectification ratio (RR) values of devices decreased with increasing light power intensity, the photocurrent values linearly improved both of the Co/Gold (III) Chloride:AuNPs /n-Si and Co/Gold (III) Chloride:AuNPs /p-Si photodiodes. According to experimental results, the obtained photodiode devices can be used for optoelectronic applications.

Declaration of Ethical Standards
The authors declare that they comply with all ethical standards.

Conflict of Interest
The authors do not have financial and personal relationships with other people or organizations that could inappropriately influence their work.

Credit Authorship Contribution Statement
Author-1: Study design, Formal analysis, Investigation, Writing – original draft, Writing – review and editing.

Data Availability Statement
All data generated or analyzed during this study are included in this published article.

5. References

Akkaya, A., B.B. Kantar, B.B., Ayyildiz , BE., Programs, T.,2019. Fabrication and characterization of Au / Carmine / N-GaAs schottky diode by spin coating technique **11** (3) (2019) 49–55, https://doi.org/10.21597/jist.942302

Akkılıç, K., Aydın, M.E., Uzun, İ., Kılıçoğlu,T.,2006. The calculation of electronic parameters of an Ag/chitin/n-Si Schottky barrier diode. Synthetic-metals, **156** (14–15) 958-962 https://doi.org/10.1016/j.synthmet.2006.06.012.

Ameline, D., Diring, S., Farre, Y., Pellegrin,Y., Naponiello,G., Blart, E., Charrier, B., Dini, D., Jacquemin, D., Odobel,F., 2015. Isoindigo derivatives for application in p-type dye sensitized solar cells. RSC Advances, **5** (2015) 85530–85539. https://doi.org/10.1039/C5RA11744E.

Aslam Manthrammel , M., Yahia, I.S., Mohd Shkir, AlFaify, S., Zahran, H.Y., Ganesh, V.,Yakuphanoglu,F., 2019. Novel design and microelectronic analysis of highly stable Au/Indigo/n-Si photodiode for optoelectronic applications. Solid State Sciences, **93**, 7-12, https://doi.org/10.1016/j.solidstatesciences.2019.04.007

Bilgili, A.K., Güzel, T., Özer,M., 2019. Current-voltage characteristics of Ag/TiO2/n-InP/ Au Schottky barrier diodes. Journal of Applied Physics, **125** (2019), 035704. https://doi.org/10.1063/1.5064637

Budak, H., Duman, S., Kaya, F.S., Ashkhasi, A., Gürbulak, B., 2020. Effect of Temperature and Illumination on the Current-Voltage Characteristics of a Al/p-GaSe/In Diode. Journal Electronic Materials, **49** (10) (2020) 5698–5704. https://doi.org/10.1007/s11664-020-08322-4.

Büchel, K.H., Moretto, H.H., Werner,D.,2008. Industrial Inorganic Chemistry Book, John Wiley & Sons, 2008.

Cavusoglu H, Akbar, H.A., Sakalak, H., Koçyiğit, A., Durmaz, F., Yıldırım, M., 2024. Investigation of the Influence of Au (Gold) Doping Concentration on the Structural, Morphological, Optical, and Electrical Parameters of an Al/Au:CuO/n-Si Heterojunction Device. Journal of Electronic Materials, **53,** 5, 2382-2397. https://doi.org/10.1007/s11664-024-10973-6

Cheung, S.K., Cheung, N.W.,1986. Extraction of Schottky diode parameters from forward current-voltage characteristics. Applied Physics Letters, **49** (1986) 85. https://doi.org/10.1063/1.97359

Clark, E.S., Templeton, D.H., MacGillavry, C.H., 1958. The crystal structure of gold (III) chloride. Acta Crystallographica, **11** (4), 284-288, https://doi.org/10.1107/S0365110X58000694.

Coetzee, D., Venkataraman, M., Militky, J., M. Petru, M., 2020. Influence of nanoparticleson thermal and electrical conductivity of composites. Polymers (Basel) , **12,** 742.
http://dx.doi.org/10.3390/polym12040742

Ejderha, K., Yıldırım, N., Abay, B., Turut, A., 2009. Examination by interfacial layer and inhomogeneous barrier height of temperature-dependent I–V characteristics in Co/p-InP contacts. Journal of Alloys Compounds, **484** (2009) 870–876.
https://doi.org/10.1016/J.JALLCOM.2009.05.062

El-Nahass, M.M., Zeyada,H.M., Abd-El-Rahman,K.F., Darwish,A.A.A.,2007. Fabrication and characterization of 4-tricyanovinyl-N, N-diethylaniline/p-silicon hybrid organic-inorganic solar cells. Solar Energy Materials Solar Cells, **91** (12) (2007) 1120–1126.
https://doi.org/10.1016/j.solmat.2007.03.016

Ganesh,V., Manthrammel, M.A., Shkir, M., Yahia, I.S., Zahran, H.Y., Yakuphanoglu, F., AlFaify, S., 2018. Organic semiconductor photodiode based on indigo carmine/n-Si for optoelectronic applications. Applied Physics Materials Science Processing, **124** (6) (2018) 1–7.
https://doi.org/10.1007/s00339-018-1832-x.

Gao, X.D., Fei, G.T., Xu, S.H., Zhong,B.N., Ouyang, H.M., Li, X.H., De Zhang,L., 2019. Porous Ag/TiO2-Schottky-diode based plasmonic hot-electron photodetector with high detectivity and fast response. Nanophotonics, **8** (2019) 1247–1254.
https://doi.org/10.1515/nanoph-2019-0094.

Gayen, R.N., Bhattacharyya, S.R., Jana, P., 2014. Temperature dependent current transport of Pd/ZnO nanowire Schottky diodes. Semiconductor Science Technology, **29** (2014), 095022,
https://doi.org/10.1088/02681242/29/9/095022

Ikram, M., Imran, M., Nunzi,J.M., Bobbara, S.R., Ali, S.,Islah-u-din., 2015. Efficient and low cost inverted hybrid bulk heterojunction solar cells. The Journal of Renewable and Sustainable Energy, **7** (4) (2015) 043148.
https://doi.org/10.1063/1.4929603.

Jackle, S., Mattiza, M., Liebhaber, M., Bronstrup, G., Rommel, M., Lips, K., Christiansen, S., 2015. Junction formation and current transport mechanisms in hybrid n-Si/PEDOT:PSS solar cells. Scientific Reports, **5**, 13008;
https://doi.org/10.1038/srep13008

Kacus, H and Aydogan, S., Optical Characteristics of Au Nanoparticles and Electrical Characteristics of Au Contacts on Si by Embedded Au Nanoparticles Schottky Devices at Low Temperatures and Under the Illumination. Available at SSRN:
http://dx.doi.org/10.2139/ssrn.4265577.

Kacus, H., Metin,O., Sevim,M., Biber,M., Baltakesmez,A., Aydogan,S., 2021. A comparative study on the effect of monodisperse Au and Ag nanoparticles on the performance of organic photovoltaic devices. Optical Materials, **116** (2021) 111082.
https://doi.org/10.1016/j.optmat.2021.111082.

Kacus, H., Aydoğan, Ş., M. Biber, M., Metin, Ö., and Sevim, M., 2019. The power conversion efficiency optimization of the solar cells by doping of (Au:Ag) nanoparticles into P3HT:PCBM active layer prepared with chlorobenzene and chloroform solvents. Materials Research Express, **6** (2019) 095104,
https://doi.org/10.1088/2053-1591/ab309a

Kacus, H., Y. Sahin, Y., S. Aydogan,S., Incekara, U., Yilmaz, M., 2020. Co/aniline blue/silicon sandwich hybrid heterojunction for photodiode and low-temperature applications. Journal of Sandwich Structures and Materials, **23** (6) (2020) 109963622090994.
https://doi.org/10.1177/1099636220909946

Kacus, H., Yilmaz, M., Incekara,U., Kocyigit, A., Aydogan,S., 2021. The photosensitive activity of organic/inorganic hybrid devices based on Aniline Blue dye:Au nanoparticles (AB@Au NPs), Sensors and Actuators A, **330** (2021) 112856.
https://doi.org/10.1016/j.sna.2021.112856

Kacus, H., Yilmaz, M., Kocyigit,A., Incekara,U., S. Aydogan,S.,2020. Optoelectronic properties of Co/pentacene/Si MIS heterojunction photodiode. Physical B Condensed Matter, **597** 412408.
https://doi.org/10.1016/j.physb.2020.412408.

Kacus, H., Biber,M., Aydoğan,Ş., 2020. Role of the Au and Ag nanoparticles on organic solar cells based on P3HT: PCBM active layer. Applied Physics A, **126**, 817.
https://doi.org/10.1007/s00339-020-03992-7.

Kaplan, N., Taşcı, E., Emrullahoğlu, M., Gökce, H., Tuğluoğlu, N., Eymur, S., 2021. Analysis of illumination dependent electrical characteristics of α-styryl substituted BODIPY dye-based hybrid heterojunction. Journal of Materials Science: Materials in Electronics, **32** (12), 16738–16747.
https://doi.org/10.1007/s10854-021-06231-8.

Kelly, K.L., Coronado, E., Zhao, L.L., Schatz,G.C.,2003. The optical properties of metal nanoparticles: the influence of size, shape, and dielectric environment. Journal Physical Chemistry B, **107,** 668–677,
https://doi.org/10.1021/jp026731y.

Kocyigit, A., Yıldırım, M., Sarılmaz, A., Ozel,F., 2019. The Au/Cu2WSe4/p-Si photodiode: electrical and morphological characterization, Journal of Alloys Compounds, **780,** 186–192.
https://doi.org/10.1016/J.JALLCOM.2018.11.372.

Kocyigit, A., Yilmaz, M., Aydogan, S., Incekara,U., Kacus,H., 2021. Comparison of n and p type Si-based Schottky photodiode with interlayered Congo red dye. Materials Science in Semiconductor Processing, **135,** 106045.
https://doi.org/10.1016/j.mssp.2021.106045.

Kottmann, J.P., Martin, O.J.F., Smith, D.R., Schultz, S.,2001. Optical Properties and Applications of Shape Controlled Metal Nanostructures. Chemistry Physical Letter, **341,** 1–6. https://doi.org/10.1016/S0009-2614(01)00171-3.

Luongo, G., Giubileo, F., Genovese, L., Iemmo, L., Martucciello, N., Di Bartolomeo, A., 2017. I-V and C-V characterization of a high-responsivity graphene/silicon photodiode with embedded MOS capacitor. Nanomaterials, **7**, 158. https://doi.org/10.3390/nano7070158

Mock, J.J., Barbic, M., Smith,D.R., Schultz, D.A., Schultz, S.,2002. Shape effects in plasmon resonance of individual colloidal silver nanoparticles. Journal Chemistry Physical, **116,** 6755. https://doi.org/10.1063/1.1462610.

Norde,H., 1979. A modified forward I-V plot for Schottky diodes with high series resistance. Journal of Applied Physics, **50,** 5052–5053. https://doi.org/10.1063/1.325607

Orak, İ., Kocyiğit, A., Karataş,Ş., 2018. The analysis of the electrical and photovoltaic properties of Cr/p-Si structures using current-voltage measurements. Silicon, **10,** 2109–2116. https://doi.org/10.1007/s12633-017-9731-x.

Ozkartal, A., Ameen ,R.H., Temirci, C., Turut,A., 2019. Electrical properties of Sn/Methyl Violet/p-Si/Al Schottky diodes. Materials Today Processing, **18**, 1811–1818. https://doi.org/10.1016/j.matpr.2019.06.668.

Reem, A.W., 2018. Photocurrent and photocapacitance properties of an Al/Coumarin/p- Si/Al photodiode. Silicon, **10**(4), 1639–1643. https://doi.org/10.1007/s12633-017-9647-5.

Santos, dos C., Brum, L.F.W., F´atima Vasconcelos R., Velho, S.K., dos Santos, J.H.Z., 2018. Color and fastness of natural dyes encapsulated by a sol-gel process for dyeing natural and synthetic fibers. Journal of Sol-Gel Science and Technology, **86** (2), 351–364. https://doi.org/10.1007/s10971-018-4631-0.

Seo, K.D., Song, H.M., Lee, M.J., Pastore, M., Anselmi,C., De Angelis, F., Nazeeruddin,M.K., Gräetzel , M., Kim,H.K.,2011. Coumarin dyes containing low-band-gap chromophores for dye-sensitised solar cells. Dyes Pigments, **90** (3), 304–310. https://doi.org/10.1016/j.dyepig.2011.01.009.

Shafique,S., Yang, S., Wang, Y., Woldu, Y.T., Cheng, B., Ji, P., 2019. High-performance photodetector using urchin-like hollow spheres of vanadium pentoxide network device. Sensors Actuators:A Physics, **296,** 38–44. https://doi.org/10.1016/j.sna.2019.07.003.

Spinelli, P., Polman, A., 2012. Prospects of near-field plasmonic absorption enhancement in semiconductor materials using embedded Ag nanoparticles. Optic Express, **20,** 641–654. https://doi.org/10.1364/OE.20.00A641.

Taşçıoğlu, İ., Aydemir, U., Altındal,Ş., The explanation of barrier height inhomogeneities in Au/n-Si Schottky barrier diodes with organic thin interfacial layer. Journal of Applied Physics, **108,** 064506. https://doi.org/10.1063/1.3468376.

Tatar, B., Bulgurcuoglu, A.E., Gokdemir, P., Aydogan, P., Yilmazer, D., Özdemir,O., Kutlu, K., 2009. Electrical and photovoltaic properties of Cr/Si Schottky diodes. Int. Journal of Hydrogen Energy, **34,** 5208–5212,. https://doi.org/10.1016/j.ijhydene.2008.10.040

Tataroglu, A., Dayan,O., Ozdemir, N., Serbetci, Z.,Al-Ghamdi, A.A., Dere, A., El-Tantawy, F., Yakuphanoglu, F., 2016. Single crystal ruthenium(II) complex dye based photodiode. Dyes Pigments, **132**, 64-71. https://doi.org/10.1016/j.dyepig.2016.04.044.

Yildiz, D.E., Gullu, H.H., Sarilmaz, A., Ozel,F., Kocyigit, A., Yildirim,M., 2020. Dark and illuminated electrical characteristics of Si-based photodiode interlayered with CuCo5S8 nanocrystals. Journal Materials of Science: Materials in Electronics, **31,** 935–948. https://doi.org/10.1007/s10854-019-02603-3.

Yilmaz, M., Kocyigit, A., Cirak,B.B., Kacus, H., Incekara, U., Aydogan,S., 2020. The comparison of Co/hematoxylin/n-Si and Co/hematoxylin/p-Si devices as rectifier for a wide range temperature. Materials Science Semiconductor Processing, **113**, 105039, https://doi.org/10.1016/j.mssp.2020.105039

Yüksel,O.F., Tuğluoğlu,N., Gülveren,B., Şafak,H., Kuş, M., 2013.Electrical properties of Au/perylene-monoimide/p-Si Schottky diode. Journal of Alloys Compounds, **577,** 30–36. https://doi.org/10.1016/j.jallcom.2013.04.157.

Zandonay, R., Delatorre,R.G., A.A. Pasa, A.A., 2008. Electrical characterization of electrodeposited Co/p-Si Schottky diodes. ECS Transactions, **14,** 359–363. https://doi.org/10.1149/1.2956050.

Zhang, J.Z., Noguez, C., 2008. Plasmonic optical properties and applications of metal nanostructures. Plasmonics, **3,** 127–150. https://doi.org/10.1007/s11468-008-9066-y.